Influence of silver addition on Cu_2O and its activity for carbon dioxide photoreduction

Fernanda Cristina Fraga[1*], Sarah Mozzaquatro Pasini[2], Fernanda Volpatto[3], Regina de Fátima Peralta Muniz Moreira[1]

[1]*Laboratory of Energy and Environment – LEMA, Department of Chemical and Food Engineering – EQA, Federal University of Santa Catarina – UFSC, Florianópolis, Brazil, fragafernandac@gmail.com*

[2]*Interdisciplinary Laboratory for the Development of Nanostructures (LINDEN), Department of Chemical and Food Engineering – EQA, Federal University of Santa Catarina – UFSC, Florianópolis, Brazil.*

[3]*Analysis Center of the Department of Chemical and Food Engineering, Department of Chemical and Food Engineering – EQA, Federal University of Santa Catarina – UFSC, Florianópolis, Brazil*

Resumo/Abstract

RESUMO - A captura, o armazenamento e a utilização do dióxido de carbono (CO_2) têm sido amplamente investigadas, devido ao efeito no ambiente do aumento da concentração desse gás. Dentre as diferentes tecnologias de utilização do CO_2, a redução fotocatalítica tem se destacado pela possibilidade de obtenção de combustíveis renováveis, como o metano. Este processo ainda depende da disponibilidade de um fotocatalisador competitivo frente a outras tecnologias de redução do CO_2. Assim, este trabalho aborda a influência da adição de diferentes porcentagens de prata (0, 4, 12 e 20% m/m) em Cu_2O na atividade fotocatalítica e produção de metano a partir da redução fotocatalítica do CO_2. Os testes foram conduzidos sob radiação UV-A e 20 °C em sistema de fluxo contínuo. Os catalisadores sintetizados foram caracterizados por DRX, FTIR, MEV-FEG e refletância difusa. A presença de prata garantiu a redução da energia de *band gap* dos compostos bimetálicos, indicando atividade na região visível. Além disso, somente os catalisadores bimetálicos foram ativos na fotorredução do CO_2, o que pode ser associado com a atuação da prata como co-catalisador, reduzindo assim a recombinação das cargas fotogeradas.

Palavras-chave: catalisadores, dióxido de carbono, metano

ABSTRACT - The capture, storage, and utilization of carbon dioxide (CO_2) have been widely investigated due to the impact of increased concentrations of this gas on environment. Among the various CO_2 technologies, photocatalytic reduction has been highlighted for its potential to generate renewable fuels, such as methane. This process still relies on the availability of a photocatalyst that is competitive with other CO_2 reduction technologies. Thus, this study investigates the influence of adding different silver percentages (0, 4, 12, and 20 wt%) in Cu_2O on the photocatalytic activity and methane production via CO_2 photocatalytic reduction. The tests were conducted under UV-A radiation at 20 °C in a continuous flow system. The synthesized catalysts were characterized by XRD, FTIR, FEG-SEM and diffuse reflectance. The presence of silver ensured a reduction in the band gap energy of the bimetallic compounds, indicating activity in the visible light spectrum. Moreover, only the bimetallic catalysts were active in the photocatalytic reduction of CO_2, which can be attributed to the role of silver as a co-catalyst, reducing the recombination of photogenerated electrons.

Keywords: catalyst, carbon dioxide, methane.

Introduction

The increase in CO_2 concentration in the atmosphere has raised serious concerns about global warming. This has triggered the proposal of various strategies to control CO_2 concentration in recent decades, driving the search for technologies to capture, store, and utilize it. As a result, the development of new materials and different strategies for utilizing recovered CO_2 has gained significant attention (1).

Artificial photosynthesis uses solar energy to convert CO_2 and H_2O into useful chemicals and is a key strategy for carbon neutrality. However, artificial photosynthesis is still an emerging technology and has been limited by the lack of catalysts with sufficient activity for large-scale demonstration. In recent studies, it has been demonstrated that the presence of silver nanoparticles supported on different semiconductors can enrich the photogenerated electrons originating from visible light-driven Cu_2O octahedral nanocrystals (2). However, no deep study has demonstrated the effect of silver nanoparticles on semiconductors in photocatalytic methane production.

In this study, photocatalysts with varying theoretical silver contents (0, 4, 12, and 20% w/w) on Cu_2O were synthesized and deeply characterized. The photocatalytic

CO_2 photoreduction under UV-A illumination at room temperature was also investigated.

Experimental

Materials

All the chemical reagents used in the experiments were of analytical grade and used without any purification treatment: polyvinylpyrrolidone – PVP (K-30, 96%, Dinâmica), copper chloride dihydrate (99%, Vetec), sodium hydroxide (97%, Neon), ascorbic acid (99%, Neon), sodium borohydride (98%, Dinâmica), silver nitrate (99%, Sigma), ethanol (98%, Dinâmica), carbon dioxide (99,99%, White Martins).

Cu_2O synthesis

The synthesis of copper oxide was adapted from literature (3). Here, 3.333g of PVP were added to 100 mL of aqueous $CuCl_2.2\ H_2O$ solution (0.01 $mol.L^{-1}$) until completely homogenized. Next, 10 mL of NaOH solution (2.0 mol. L^{-1}) was added drop by drop. After 30 minutes, 10 mL of a solution of ascorbic acid (0.6 $mol.L^{-1}$) was added drop by drop. After 3 hours of stirring and heating, the solids were collected by centrifugation (7500 rpm, 5 minutes), washed with deionized water and ethanol, and dried in an oven at 60 °C overnight to obtain Cu_2O particles.

Ag/Cu_2O synthesis

For silver doping, the methodology adapted from Tang and collaborators (2) was used. For this, the methodology described above for the synthesis of copper oxide was repeated, but before centrifugation, 20 mL of $NaBH_4$ solution and 20 mL of an $AgNO_3$ solution (1 mol:1 mol) were added simultaneously and slowly. The resulting solution was kept under magnetic stirring for 3 hours, and the solids were collected and washed as described above. Materials with 4, 12, and 20% of the theoretical mass of silver were prepared, denominated $4Ag/Cu_2O$, $12Ag/Cu_2O$, and $20Ag/Cu_2O$, respectively.

Characterization

The synthesized particles were characterized by X-ray diffraction (Rigaku MiniFlex600), with CuKα radiation (λ = 0,15406 nm), a potential difference of 40 kV during operation, and an electric current of 15 mA, in the range of 20 to 90°. The chemical bonds were identified using Fourier transform infrared spectroscopy (Spectrum Two – Perkin Elmer), at wavenumbers between 4000 and 550 cm^{-1}. The band gap energy (Eg) was estimated by reflectance analysis and obtaining the Kubelka-Munk function in a UV-Vis-NIR spectrophotometer (UV-3600i Plus, Shimadzu) equipped with an integrating sphere, scanning in the 750 to 200 nm range, reflectance measurements every 1.0 nm and fast analysis speed. The morphology of the samples was investigated by field emission gun scanning electron microscopy (FEG-SEM, JEOL JSM-6701F).

CO_2 photoreduction

A schematic representation of the reaction system to investigate the reaction between carbon dioxide and water is shown in Figure 1. For the tests, 350 mL of deionized and deoxygenated water was boiled, placed in the reactor (with only one inlet and one outlet), kept under constant magnetic stirring and with CO_2 bubbling at a flow rate of 15 $mL.min^{-1}$, with a thermostatic bath with recirculation turned on, guaranteeing the cooling of the water and a constant temperature of 20 °C during the experiment (4). The catalyst (0.4 $g.L^{-1}$) was then added and, after 3 hours of saturation, the Hg lamp (120 W) was turned on and the output current was monitored to observe the formation of the products (CO and CH_4) and the reminiscent CO_2 concentration.

The photocatalytic activity was investigated by taking gas samples and injecting them into a gas chromatograph (GC2014, Shimadzu) with FID/TCD detectors and methanator, using a Carboxen^{TM} 1000 60/80 packed column (Supelco®), with argon (99.999%, White Martins) as the carrier gas. A 100 µL gas sample was injected every 20 minutes, and the chromatograph was previously calibrated using a mixture of standard gases (4.0% CH_4, 4.0% CO, and 4.0% CO_2).

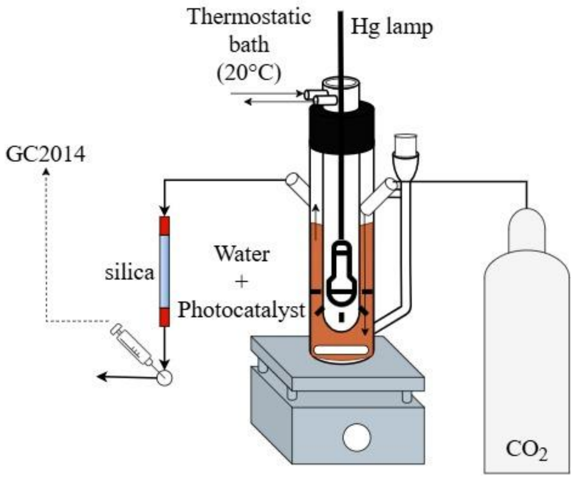

Figure 1. Schematic representation of the reaction system.

Results and Discussion

The results of XRD analysis are shown in Figure 2. The formation of crystalline structures is observed, with six characteristic peaks of the octahedral Cu_2O: 29.6, 36.4, 42.3, 61.3, 73.5 and 77.3°, approximately, attributed to the cubic phase facets (1 1 0), (1 1 1), (2 0 0), (2 2 0), (3 1 1) and (2 2 2), respectively (JCPDS nº 05–0667). It is possible to identify the presence of Ag with characteristic peaks at approximately 38°, attributed to the (1 1 1) facet of the cubic phase of the silver particles (JCPDS no. 04-0783).

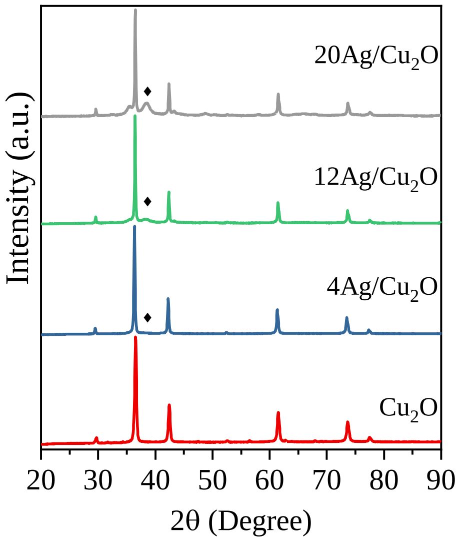

Figura 2. X-ray diffractogram of Cu_2O (red), 4Ag/Cu_2O (blue), 12Ag/Cu_2O (green), and 20Ag/Cu_2O (gray).

The FTIR spectra of the synthesized particles are shown in Figure 3. The samples exhibit a strong vibrational band, located at 632 cm^{-1}, which is attributed to the stretching vibration characteristic of the Cu(I)-O bond in the Cu_2O phase (5). The bands around 3500 and 1620 cm^{-1} are attributed to the bending vibration of -OH groups, resulting from the adsorption of water molecules on the catalyst surface (2).

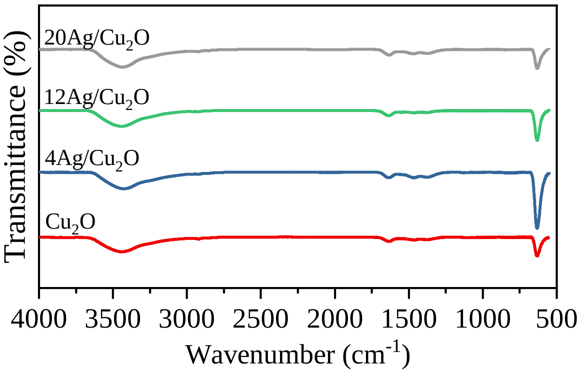

Figure 3. FTIR spectra of Cu_2O (red), 4Ag/Cu_2O (blue), 12Ag/Cu_2O (green), and 20Ag/Cu_2O (gray).

The UV-vis absorbance spectra are shown in Figure 4a. All the synthesized samples absorb in the visible region (400–700 nm), indicating the potential activation of these photocatalysts within this range. Reflectance spectroscopy analysis was performed to analyze the optical properties of the synthesized materials. Considering the direct transition for Cu_2O compounds (5), and extrapolating the Tauc plot, the Eg values were estimated, as shown in Figure 4b. These values are summarized in Table 1, where a reduction in Eg values due to the presence of silver particles can be observed.

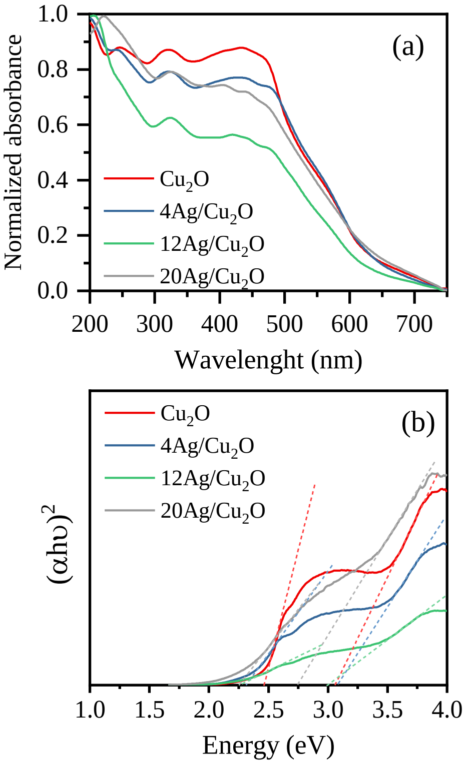

Figure 4. Absorbance spectra (a) and Tauc plot for estimating the band gap energy of Cu_2O (red), 4Ag/Cu_2O (blue), 12Ag/Cu_2O (green), and 20Ag/Cu_2O (gray).

Figure 5 shows the FEG-SEM images of the Cu_2O (a), 4Ag/Cu_2O (b), 12Ag/Cu_2O (c), and 20Ag/Cu_2O (d) samples, at 10,000x magnification. The presence of agglomerated Ag particles and Cu_2O octahedrons can be identified. Additionally, the particles are highly heterogeneous, which may be attributed to the synthesis method used (precipitation) and the modifications made to the silver deposition process. These results indicate the successful formation of the desired structures.

Moreover, FEG-SEM images (Figure 5d) reveal a more uniform dispersion of Ag particles on the material's surface, further contributing to the improved photocatalytic performance.

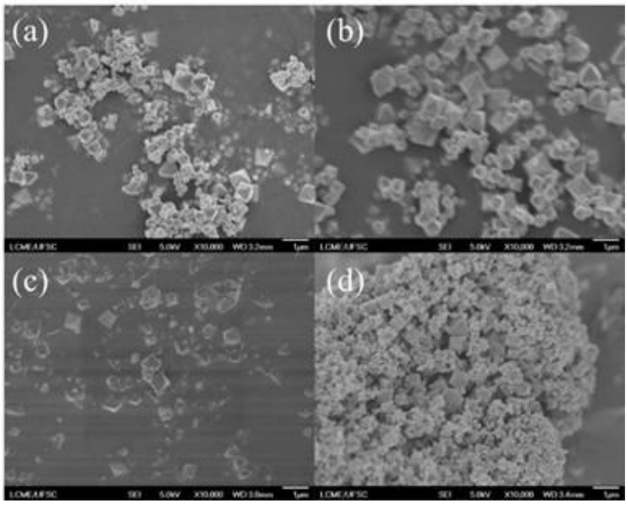

Figure 5. FEG-SEM images of Cu_2O (a), $4Ag/Cu_2O$ (b), $12Ag/Cu_2O$ (c), and $20Ag/Cu_2O$ (d).

The results of CO_2 photoreduction are expressed in production rates of the analyzed compounds (Table 1), considering a differential reactor due to the low conversion value (6). It is observed that the absence of silver on the catalyst negatively affects the CO_2 photoreduction. Furthermore, the increase in silver content resulted in higher CO and CH_4 production rates, suggesting that Ag acts as a co-catalyst (2), by capturing electrons and forming a barrier at the $Ag\text{-}Cu_2O$ interface, thereby reducing the recombination of photogenerated charge carriers. As expected, supported Ag particles with low Fermi energy can enrich the photogenerated electrons originating from visible light-driven Cu_2O octahedral nanocrystals.

Table 1. Estimated band gap energy of synthesized compounds and production rates of photocatalytic reactions.

Material	Eg (eV)	CH_4 production rate ($\times 10^{-2}$ $\mu mol.g^{-1}.min^{-1}$)	CO production rate ($\times 10^{-2}$ $\mu mol.g^{-1}.min^{-1}$)
Cu_2O	2.47; 3.05	1.1 ± 0.9	-
$4Ag/Cu_2O$	2.31; 3.08	1.8 ±0.9	8.1 ± 0.9
$12Ag/Cu_2O$	2.24; 3.00	4.1 ± 0.6	5.7 ± 0.6
$20Ag/Cu_2O$	2.25; 2.74	4.9 ± 0.9	4.0 ± 0.9

Since several factors influence photocatalytic performance, a comparison between different photocatalysts may be misleading, since the process conditions are different: continuous or batch system, the area exposed to light and the type of radiation source used, for example (7). However, results in the same order of magnitude are found in the literature. For example, Wang and collaborators (8) obtained highest production rate of CH_4 of 2.9×10^{-2} $\mu mol.L^{-1}.min^{-1}$ using $0.5Ag\text{-}0.5Cu_2O/TiO_2$ as photocatalyst.

The $4Ag/Cu_2O$ photocatalyst exhibited an enhanced CO production rate, while an increase in the Ag content corresponded to a higher CH_4 production. Accordingly, the $20Ag/Cu_2O$ sample demonstrated the highest CH_4 production rate, which can be attributed to the Ag particles on the Cu_2O nanocrystals that facilitate the reduction of CO_2 to CH_4 (2). These results agree with the photocatalytic mechanism for CO_2 photoreduction proposed by Tang and collaborators (2) (Equations 1 – 7).

$$CO_2 + e^- + H^+ \rightarrow COOH^{\bullet} \qquad (1)$$
$$COOH^{\bullet} + e^- + H^+ \rightarrow CO^{\bullet} + H_2O \qquad (2)$$
$$CO^{\bullet} \rightarrow CO_{(g)} \qquad (3)$$
$$CO^{\bullet} + e^- + H^+ \rightarrow CHO^{\bullet} \qquad (4)$$
$$CHO^{\bullet} + 2\,e^- + 2\,H^+ \rightarrow OCH_3^{\bullet} \qquad (5)$$
$$OCH_3^{\bullet} + e^- + H^+ \rightarrow CH_{4(g)} + O^{\bullet} \qquad (6)$$
$$O^{\bullet} + 2\,e^- + 2\,H^+ \rightarrow H_2O \qquad (7)$$

The Ag/Cu_2O photocatalyst with a narrower band gap can achieve higher photon enrichment. Under UV-A light irradiation, Cu_2O can absorb the photons and are excited to form the conduction band and valence band. The photogenerated electrons located at the conduction band could quickly transfer to supported Ag particles to catalytically reduce CO_2 to CO and methane.

Conclusion

In this work, Cu_2O photocatalysts doped with different silver contents (0, 4, 12, and 20%) were developed. The XRD spectra shows the presence of silver in the $12Ag/Cu_2O$ and $20Ag/Cu_2O$ compounds, as also confirmed by FEG-SEM images. The presence of silver contributed to the reduction of the band gap energy of the synthesized compounds, indicating their activity in the visible range. Furthermore, silver played a key role in the reduction of CO_2 to methane, with the sample $20Ag/Cu_2O$ exhibiting the highest production rate (4.9×10^{-2} $\mu mol.L^{-1}.min^{-1}$). This can be associated with the role of Ag as a co-catalyst, capturing electrons and forming a barrier at the $Ag\text{-}Cu_2O$ interface, thus reducing the recombination of photogenerated electrons.

Acknowledgements

The authors are grateful to the National Council for Scientific and Technological Development (CNPq) (Grant 153806/2024-9), and INCT-CAPICUA (Grant 406710/2022-8). They also acknowledge the Analysis

Center of the Department of Chemical and Food Engineering, the Central Laboratory of Electronic Microscopy (LCME-UFSC), and the Interdisciplinary Laboratory of the Development of Nanostructures (LINDEN-UFSC) for technical support.

Reference

1. X. Duan; G. Song; G. Lu; Y. Wang; J. Sun; A. Chen; X. Xie, *Mater. Today Sustain.* **2023**, *23*.
2. Z. Tang; W. He; Y. Wang; Y. Wei; X. Yu; J. Xiong; X. Wang; X. Zhang; Z. Zhao; J. Liu, *Appl. Catal. B Environ*. **2022**, *311*, 121371.
3. D.F. Zhang; H. Zhang; L. Guo; K. Zheng; X.D. Han; Z. Zhang, *J. Mater. Chem*. **2009**, *19*, 5220–5225.
4. M.I. Ostad; M.N. Shahrak; F. Galli; *J. CO2 Util*. **2021**, *43*, 101373.
5. M. Balık; V. Bulut; I.Y. Erdogan, *Int. J. Hydrogen Energy*, **2019**, *44*, 18744–18755.
6. H. S. Fogler; *Elements of Chemical Reaction Engineering*, 5th Ed.; Prentice Hall, Philadelphia, 2016.
7. S. Ali; M.C. Flores; A. Razzaq; S. Sorcar, C.B. Hiragond; H.R. Kim; Y.H. Park; Y. Hwang; H.S. Kim; H. Kim; E.H. Gong; J. Lee; D. Kim; S. In, *Catalysts*. **2019**, *9*, 1–26.
8. X. Wang; Z. Jiang; H. Chen; K. Wang; X. Wang; *J. Alloys Compd*. **2022**, *896*, 163030.